Ultra-high pressure aluminous titanites in carbonate-bearing eclogites at Shuanghe in Dabieshan, central China

D. A. CARSWELL

Department of Earth Sciences, University of Sheffield, Sheffield S3 7HF, UK

R. N. WILSON

Department of Geology, University of Leicester, Leicester LE1 7RH, UK

AND

M. ZHAI

Institute of Geology, Academia Sinica, P.O. Box 634, Beijing 100029, China

Abstract

Petrographic features and compositions of titanites in eclogites within the ultra-high pressure metamorphic terrane in central Dabieshan are documented and phase equilibria and thermobarometric implications discussed. Carbonate-bearing eclogite pods in marble at Shuanghe contain primary metamorphic aluminous titanites, with up to 39 mol.% $Ca(Al,Fe^{3+})FSiO_4$ component. These titanites formed as part of a coesite-bearing eclogite assemblage and thus provide the first direct petrographic evidence that $AlFTi_{-1}O_{-1}$ substitution extends the stability of titanite, relative to rutile plus carbonate, to pressures within the coesite stability field. However, it is emphasised that Al and F contents of such titanites do not provide a simple thermobarometric index of P–T conditions but are constrained by the activity of fluorine, relative to CO_2, in metamorphic fluids – as signalled by observations of zoning features in these titanites.

These ultra-high pressure titanites show unusual breakdown features developed under more H_2O-rich amphibolite-facies conditions during exhumation of these rocks. In some samples aluminous titanites have been replaced by ilmenite plus amphibole symplectites, in others by symplectitic intergrowths of secondary, lower Al and F, titanite plus plagioclase. Most other coesite-bearing eclogite samples in the central Dabieshan terrane contain peak assemblage rutile often partly replaced by grain clusters of secondary titanites with customary low Al and F contents.

KEYWORDS: ultra-high pressure metamorphism, titanites, eclogites, Dabieshan, China.

Introduction

PETROGRAPHIC observations indicate that rutile, rather than titanite, is the principal titanium-bearing mineral phase stabilised at 'peak' metamorphic conditions in the majority of eclogites (e.g. Mottana *et al.*, 1990, Table 2.2). In such rocks titanite frequently forms as a replacement phase around rutile during the development of the retrograde, amphibolite-facies, assemblage of hornblende + plagioclase + epidote + titanite from an eclogite-facies assemblage of garnet + omphacite + rutile + quartz.

Manning and Bohlen (1991) have emphased the high pressures required to stabilise the assemblage grossular + rutile + quartz + H_2O relative to titanite + zoisite. However, their calculations, involving the thermodynamic data base of Berman (1988), indicated that for the pure end-member reaction the titanite + zoisite stability field can be expected to extend to pressures >34 kbar, well within the coesite (rather than quartz) stability field.

Smith (1977, 1988) reported the occurrence of primary titanite in an eclogite pod at Liset, western Norway, and drew attention to its distinctive high-

Mineralogical Magazine, June 1996, Vol. 60, pp. 461–471

aluminium content. In addition Smith (1981) presented some preliminary experimental data to support the contention that the octahedral Al content in titanite, controlled by the coupled substitution $Al^{VI}(OH,F)Ti_{-1}O_{-1}$, increases with pressure and decreases with temperature.

Such 'high-aluminium' titanites, with $X_{Al} = Al/(Al + Ti + Fe^{3+}) \geqslant 0.25$ (Oberti *et al.*, 1991), have since been reported from eclogites and associated rocks in several other high-pressure metamorphic terranes (e.g. Franz and Spear, 1985; Sobolev and Shatsky, 1990; Oberti *et al.*, 1991; Hirajima *et al.*, 1992). On the other hand, Enami *et al.* (1993) have demonstrated the existence of aluminous titanites in low-grade metasediments from the Salton Sea geothermal system, USA and in granitoids and associated fluorite-bearing skarns from southwest Japan. Their study indicates that it is important to discriminate between $(OH)^-$ and F^- substitutions in titanites and hence to recognise separate, theoretical, hydroxy-titanite $[Ca(Al,Fe^{3+})(OH)SiO_4]$ and fluor-titanite $[Ca(Al,Fe^{3+})FSiO_4]$ end-member components.

According to Enami *et al.* (1993), the $(Al,Fe^{3+})(OH)Ti_{-1}O_{-1}$ substitution resulting in aluminous titanites with high hydroxy-titanite component is favoured by low temperature conditions, as for example in the titanites found in the low-temperature Salton Sea metasandstones. On the other hand, it was suggested that (Al,Fe^{3+}) F Ti_{-1} O_{-1} substitution widens the temperature stability field of titanite at high pressures, consistent with occurrences in eclogites of titanites with significant fluor-titanite component.

This paper documents and discusses occurrences of 'peak' assemblage high-aluminium titanites in carbonate-bearing eclogites from the Dabieshan collision belt in central China. As certain samples contain inclusions within garnets of both high-aluminium titanites and coesites (or their poly-crystalline quartz replacement pseudomorphs), this study provides conclusive petrographic evidence that the stability field of such high-aluminium titanites extends to the ultra-high pressure (UHP) conditions required for the stability of coesite-bearing eclogites.

Petrography

The four aluminous titanite-bearing eclogite samples (CD28, 29, 30 and 74), which are the principal subject of this paper, were all collected from small (*ca.* 0.2–1 m sized) pods within marble at a locality referred to by the Chinese as Shuanghe, about 15 km west of the county town of Qianshan in Anhui Province. A general account of the field relationships at Shuanghe, which lies close to the eastern margin of the Central Dabieshan Ultra-High Pressure Eclogite Terrane, has been provided by Cong *et al.* (1995).

FIG. 1. Field photograph of locality for pods of 'high-aluminium' titanite- and carbonate-bearing eclogite in marble at Shuanghe, Dabieshan, central China.

The mafic pods concerned typically only preserve relatively unretrograded eclogite-facies assemblages as cores within amphibolitic margins. Strings of pods are wrapped by a foliation in the encompassing marble (Fig.1) indicative of tectonic boudinage of original more coherent mafic layers, possibly basaltic flows or tuffs. The precise location of these eclogite pods is about 700 m north of the village of Shuanghe in a marble layer with adjacent jadeite-bearing metaquartzite (see Cong *et al.*, 1995, fig.2).

Eclogite sample CD28 has a well-developed retrograde foliation defined by abundant pale blue-green barroisitic amphibole and elongate quartz grains, with more minor pale yellow (in thin section) phlogopitic mica [Mg/(Mg+Fe) = 0.76–0.80] and calcite. Some of the amphibole occurs as a coarse symplectite intergrowth with sodic plagioclase. Matrix omphacite has been virtually all replaced by a fine-grained symplectite (Fig. 2*a*) but relict omphacite is frequently preserved as inclusions within large garnets, as also are small (mostly < 0.15 mm), poly-crystalline quartz inclusions (Fig. 2*b*) – some with preserved coesite relics. Discrete titanite grains (up to *ca.* 0.5 mm in size) are a fairly common matrix phase (Fig. 2*a*). Optically these titanites display distinctly lower birefringence than the common 'low-aluminium' titanites in other rocks, as to be expected for titanites with reduced titanium contents (Deer *et al.*, 1992). Some grains show evidence of compositional zoning with rim overgrowth zones of lowest birefringence, reflecting further reduced Ti and higher Al contents, as also confirmed by electron microprobe studies and evidenced by the reduced reflectivity overgrowth zones in backscattered electron image photographs (Fig. 2*c–d*). In addition the margins of most titanite grains are rather irregular and corroded with clear

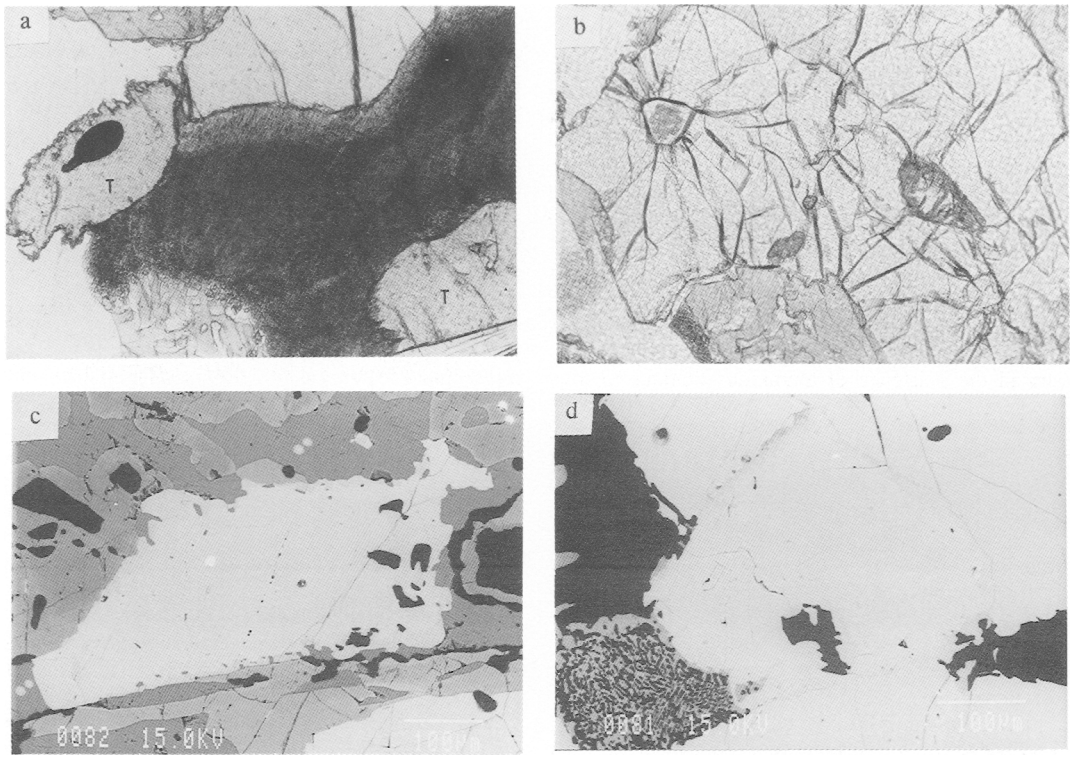

FIG. 2. Petrographic features in sample CD28 from Shuanghe. (*a*) Plane polarised light photmicrograph – *ca.* 1.2 mm. across. Note the two high relief 'primary' aluminous titanites (labelled T and one with a rutile inclusion and adjacent garnet); fine-grained symplectite after omphacite; secondary amphibole and plagioclase aggregates; relatively coarse-grained quartz. (*b*) Plane polarised photomicrograph with mostly high-relief garnet in the *ca.* 1.2 mm. field of view. Note that garnet contains relictic inclusions of omphacite (right), poly-crystalline quartz after coesite (left) and three small aluminous titanites (low centre). Amphibole-plagioclase symplectitic intergrowth is apparent external to the garnet. (*c*) Backscattered electron image of large 'primary' aluminous titanite grain (centre) showing an irregular darker outer zone with higher Al and lower Ti content and a small bright rutile inclusion. (*d*) Backscattered electron image of central 'primary' aluminous titanite grain largely enclosed in garnet and with a small bright rutile inclusion close to top of grain, a narrow edge zone of reduced reflectivity resulting from a higher Al/Ti ratio, and the initiation of breakdown reaction along the irregular top left edge. Bottom left is fine-grained symplectite after omphacite.

indications of instability and initiation of the growth of retrograde replacement products (Fig. 2*c–d*). Whilst titanites may contain small rutile inclusions (Fig. 2*b–d*), an important observation is that small titanite grains occur as common inclusions within garnets in association with omphacite and poly-crystalline quartz inclusions. Garnet grains are essentially unzoned (Fig. 3*a*) and it is concluded that these titanites grew, and equilibrated with, the ultra-high pressure, eclogite-facies mineral assemblage of garnet + omphacite + coesite.

Eclogite sample CD29 is coarser grained with garnets up to 1 cm across. It also contains much less quartz but more carbonate. Replacement blue-green amphibole is limited to reaction coronas around garnets, but matrix omphacites are again extensively replaced by fine-grained symplectite. Minor pale brown biotite mica is limited to coarser symplectite intergrowths with feldspar, considered to have replaced earlier phengite mica grains in equilibrium with the garnet + omphacite + carbonate assemblage. The predominant carbonate phase in textural equilibrium with garnet + omphacite is a ferroan dolomite, but it is usually rimmed by a later Mg-and Fe-bearing calcite. Some large garnets in this sample retain indications of limited prograde growth compositional zoning (Fig. 3*b*), with slight increases in Ca and Mg contents relative to Fe and Mn close to

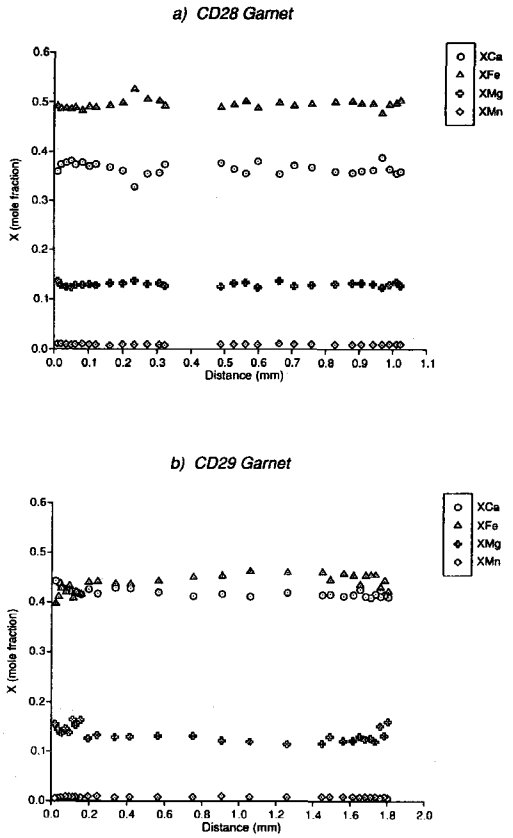

FIG. 3. Compositional zoning profiles across garnet grains in (*a*) sample CD28 and (*b*) sample CD29 from Shuanghe, Dabieshan.

grain margins. The large garnets commonly contain abundant small inclusions of omphacite, apatite and 'high-aluminium' titanite. Although the latter may again sometimes contain small rutile inclusions, there is little doubt that titanite formed as part of the eclogite-facies assemblage. Apatite is uncommonly abundant in this sample and some larger grains show unusual fine-grained exsolution under transmission light microscopy (Fig. 4*a*–*b*). As these exsolution lamellae are not apparent in backscattered electron images and electron microprobe observations failed to establish the presence of a phase with substantially different composition, the exsolution may just involve apatites with different fluorine contents (3.8–4.9 wt.% F detected). The larger matrix titanites in this sample mostly show at least partial replacement by a semi-opaque phase intergrowth (Fig. 4*a*–*b*) which can be readily resolved in backscattered electron images (Fig. 4*c*–*d*). The dominant phases replacing the 'high-aluminium' titanite are ilmenite and amphibole but minor albitic plagioclase and calcite may also occur within the replacement symplectite.

Eclogite sample CD30 is similar in most respects to sample CD29. Although uniformly finer-grained than CD29, it again lacks a foliation and, other than for the matrix omphacite, the eclogite-facies minerals are mostly well preserved. Secondary biotite mica is lacking in this sample and there is thus no evidence in this case of earlier phengite. 'High-aluminium' titanites again occur both as inclusions within garnets and as larger matrix grains, showing similar replacement features as in CD29 (see Fig. 4). Apatite is less common, but some grains again show the unusual exsolution feature noted in CD29. Iron sulphide grains (pyrite) are a more conspicuous accessory in this sample and some contain inclusions of 'high-aluminium' titanite and zircon. Two carbonate phases are again present with earlier ferroan dolomite again enclosed in Fe- and Mg-bearing calcite.

Eclogite sample CD74 shows a number of different features related to the fact that retrogression and recrystallization to an amphibolite-facies assemblage is most advanced in this sample, although only a weak foliation has developed. In particular the large (up to *ca.* 0.4 mm) irregularly-shaped titanite grains present show rather different breakdown features. These titanite grains retain parts with 'high-aluminium' titanite compositions. However, these Al-rich, Ti-reduced grains, with relatively low birefringence and reflectivity, have been partly replaced by secondary titanite with higher birefringence and reflectivity, reflecting lower Al and higher Ti contents. This secondary titanite is intergrown with some vermicular-textured plagioclase (Fig. 5*a*–*b*). Small rutiles are more common in this sample, occurring both within the titanites and enclosed directly within garnets, as also are some titanite grains. Omphacite in this sample has been entirely replaced by a coarse-grained symplectite of pargasitic amphibole and sodic plagioclase, and secondary aegerine-augite grain coronas occur around some quartz grains. Some garnets in this sample have been completely replaced by coarse-grained amphibole + clinozoisite/epidote intergrowths.

Eclogite samples CD18-1, 18-2, 40 and 41. For comparative purposes, analyses of secondary 'low-aluminium' titanites in four other samples from the Central Dabieshan UHP Eclogite Terrane have also been included in this study. Samples CD18-1 and 18-2 are heavily retrograded eclogites from pods within quartzo-feldspathic gneisses in the river section close to Shima village. Samples CD40 and 41 are from rather less retrograded carbonate-bearing eclogite pods in marble at a locality called

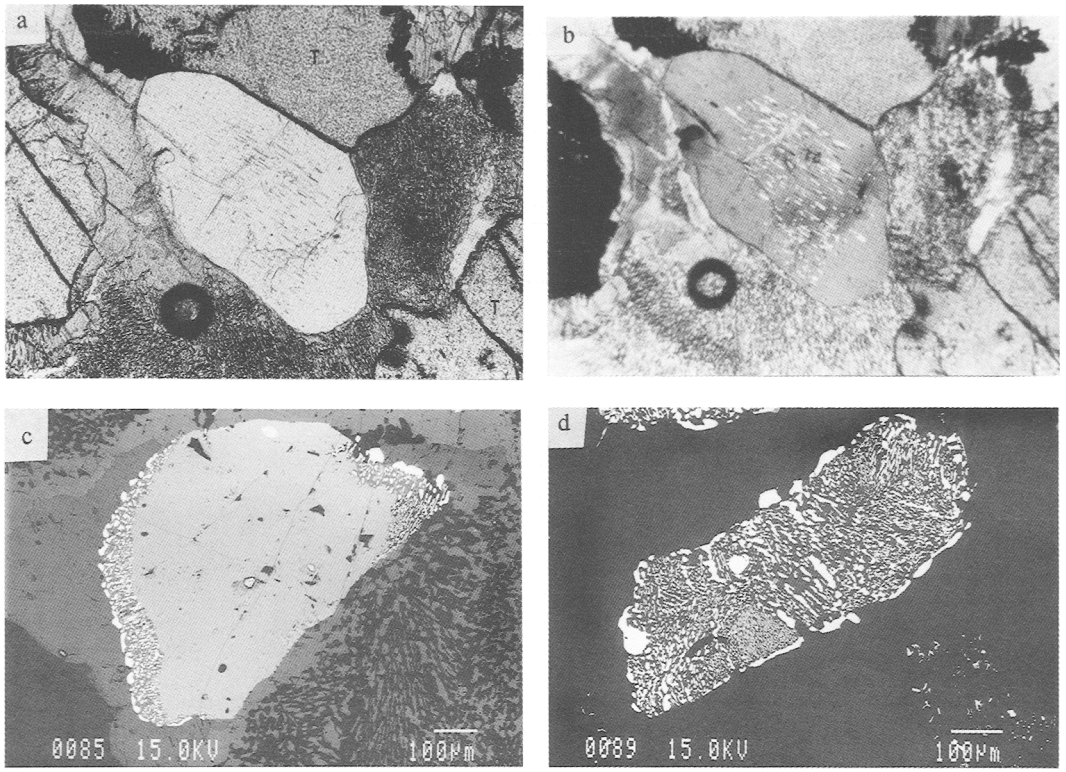

FIG. 4. Petrographic features in sample CD29 from Shuanghe. Plane polarised light (*a*) and crossed polarised light (*b*) photomicrographs *ca.* 1.2 mm across. Note the central apatite grain with exsolution ; two high-relief aluminous titanite grains (labelled T and one with conspicuous semi-opaque breakdown rim); symplectite after omphacite; secondary amphibole + plagioclase aggregates; and garnet grain (left). (*c*) Backscattered electron image of 'primary' aluminous titanite with partial edge replacement by a symplectite of ilmenite (bright) and amphibole (darker). Note the high reflectivity rutile inclusion towards top of titanite grain. (*d*) Backscattered electron image of aluminous titanite grain completely replaced by symplectite of ilmenite (bright) and amphibole (darker) plus minor plagioclase and calcite.

Guanjialing. The last two samples contain within garnets some clear relict coesite inclusions, part replaced by polycrystalline quartz aggregates, as well as clusters of titanite grains replacing earlier rutiles (Fig. 5*c*–*d*) – the characteristic textural relationship of such secondary titanites relative to rutiles in these and many other eclogite samples.

Titanite compositions

Mineral compositions were obtained on the JEOL JXA-8600 S microprobe in the Department of Geology at the University of Leicester, using wavelength-dispersive analysis and an acceleration voltage of 15 kV. A special analysis procedure which included determination of Zr, Nb, La, Ce, Y and F contents was set up for these titanites. Minimum detection limits and 2σ errors (as % oxides) for these analyses, as calculated from the counting statistics, are indicated in the last two columns of Table 1. Analyses of the early UHP eclogite-facies titanites are listed in Table 1 and analyses of secondary amphibolite-facies titanites in Table 2. For each sample and titanite type, analyses with maximum and minimum determined aluminium contents are listed. On the other hand, all determined point analyses of each titanite type in each sample are plotted in Figs. 6 and 7.

As recognised by previous workers (e.g. Smith, 1981; Franz and Spear, 1985; Enami *et al.*, 1993) and evidenced by strong negative linear correlations on Ti *vs.* (Al,Fe^{3+}) plots (Fig. 6) and positive correlations on F *vs.* (Al,Fe^{3+}) plots (Fig. 7), variations in Al and Fe contents in titanites can be largely attributed

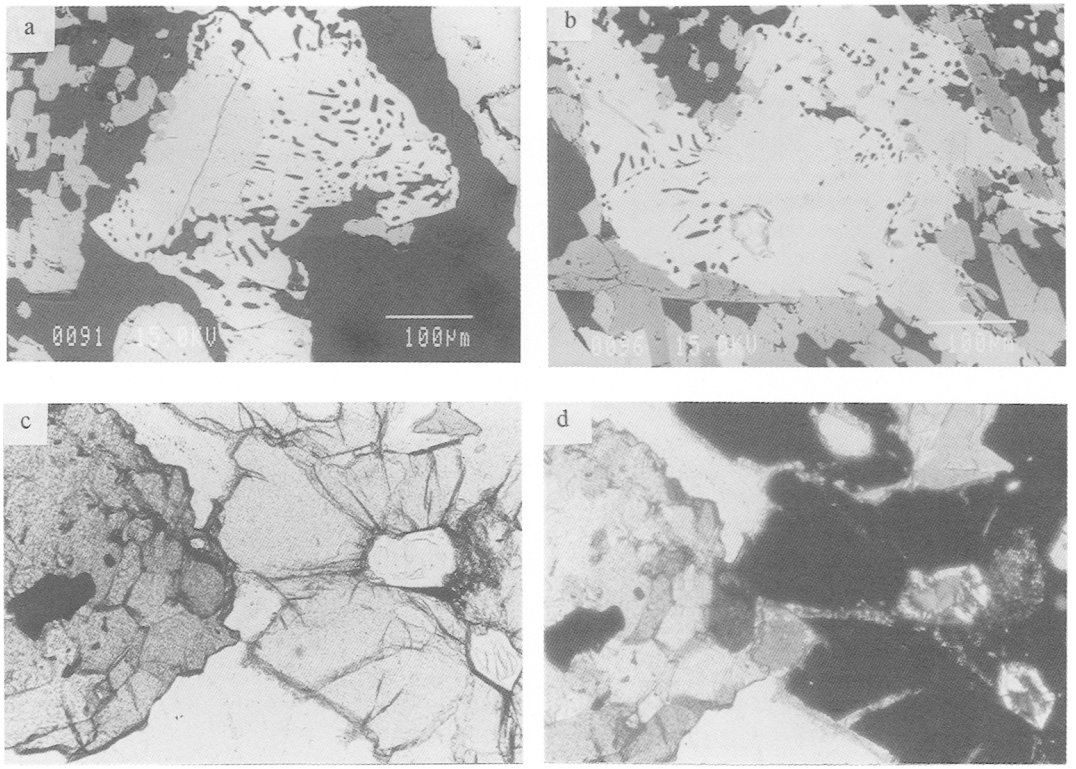

FIG. 5. Petrographic features in samples CD74 and CD41. (*a*) Backscattered electron image of titanite grain in sample CD74 showing a "high-aluminium" titanite relictic portion (left centre with lower reflectivity) within a replacement symplectite of lower aluminium secondary titanite and vermicular plagioclase (darker phase). (*b*) Backscattered electron image of very irregular shaped titanite grain in sample CD74 with part preserved original 'high-aluminium' composition with lower reflectivity (centre and right) and replacement titanite of higher reflectivity intergrown with some vermicular plagioclase. Adjacent grains are mostly calcic amphibole (dark grey) and plagioclase (dark). Plane polarised light (*c*) and crossed polarised light (*d*) photomicrographs *ca.* 1.2 mm across of sample CD41 showing a large secondary titanite grain cluster around earlier rutile. Also note the two coesite inclusions within garnet occurring as central higher relief relics within poly-crystalline quartz replacement aggregrates.

to the coupled substitutions:

$$Ti^{4+} + O^{2-} = (Al,Fe^{3+}) + (F,OH)^{-}$$

The Al^{3+} cations, which usually predominate over Fe^{3+} in natural titanites, thus occur in octahedral sites whereas rare earth elements may substitute for Ca^{2+}. The $(OH)^{-}$ and F^{-} anions can replace O^{2-} anions in the one out of every five sites not bound to any of the SiO_4 groups.

In view of the variable oxygen content of these titanites it is inappropriate to calculate a structural formula on the basis of five oxygens, as for ideal titanite ($CaTiSiO_5$). Instead the structural formulae in Tables 1 and 2 have been calculated on the basis of three total cations, in the manner proposed by Franz and Spear (1985). An assumption has been made that all iron is present as Fe^{3+} and, as H_2O contents have not been analytically determined, the (OH) contents have been calculated as $(OH) = (Al + Fe^{3+}) - F$. This assumes that all Al^{3+} and Fe^{3+} is coupled to either F^{-} or $(OH)^{-}$ anions as in the above substitution equation.

The number of oxygen anions has been calculated by charge balance considerations as Oxygens = 0.5 [(sum of cation charges) − OH − F]. For the listed titanite analyses in Tables 1 and 2, the sums of (Ti + Al + Fe) are in the range 0.989–1.001 and of (OH + F + O) in the range 4.979–4.999 (close to ideal values of 1.0 and 5.0, respectively), so supporting the stoichiometric assumptions made.

TABLE 1. Microprobe analyses and calculated structural formulae to three total cations for 'primary' ultra-high pressure titanites in Dabieshan eclogites

Sample Number	CD 28	CD 28	CD 29	CD 29	CD 30	CD 30	CD 74	CD 74	Min Detect. Limit	2σ Error
Al_2O_3 content	Max	Min	Max	Min	Max	Min	Max	Min		
Wt.%										
SiO_2	31.29	31.07	31.31	31.09	31.29	31.13	31.15	31.15	0.023	0.17
TiO_2	21.40	30.45	26.99	32.08	27.56	30.27	28.50	29.67	0.031	0.27
Al_2O_3	12.72	6.79	8.93	5.44	8.75	6.65	7.96	7.31	0.016	0.05
Fe_2O_3	0.40	0.41	0.34	0.60	0.38	0.49	0.34	0.38	0.047	0.06
MnO	0.03	0.03	0.02	0.03	0.01	0.00	0.03	0.03	0.047	0.04
MgO	0.07	0.08	0.08	0.03	0.11	0.10	0.07	0.08	0.013	0.02
CaO	29.08	29.24	29.18	29.35	29.82	29.39	29.55	29.53	0.030	0.26
Na_2O	0.02	0.07	0.07	0.03	0.06	0.08	0.07	0.08	0.015	0.02
K_2O	0.00	0.01	0.01	0.01	0.01	0.00	0.01	0.00	0.022	0.02
ZrO_2	0.02	0.06	0.01	0.06	0.06	0.00	0.02	0.01	0.073	0.09
Nb_2O_5	0.01	0.06	0.02	0.05	0.05	0.06	0.04	0.06	0.074	0.09
La_2O_3	0.06	0.17	0.18	0.18	0.03	0.06	0.17	0.01	0.165	0.19
Ce_2O_3	0.03	0.04	0.02	0.15	0.05	0.07	0.02	0.11	0.153	0.19
Y_2O_3	0.04	0.08	0.03	0.07	0.03	0.02	0.03	0.00	0.067	0.08
F	3.90	2.28	2.48	1.98	3.22	2.27	2.01	2.73	0.051	0.26
Minus O≡F	1.64	0.96	1.04	0.83	1.36	0.96	0.85	1.15		
Total	97.43	99.88	98.64	100.32	100.07	99.63	99.12	100.00		
Si	0.998	0.991	0.999	0.994	0.988	0.994	0.991	0.990		
Ti	0.513	0.730	0.647	0.771	0.655	0.727	0.682	0.709		
Al	0.478	0.255	0.336	0.205	0.326	0.250	0.299	0.274		
Fe^{3+}	0.010	0.010	0.008	0.014	0.009	0.012	0.008	0.009		
Mn	0.001	0.001	0.001	0.001	0.000	0.000	0.001	0.001		
Mg	0.003	0.004	0.004	0.001	0.005	0.005	0.003	0.004		
Ca	0.994	0.999	0.997	1.005	1.009	1.005	1.008	1.006		
Na	0.001	0.004	0.004	0.002	0.004	0.005	0.004	0.005		
K	0.000	0.000	0.000	0.000	0.000	0.000	0.000	0.000		
Zr	0.000	0.001	0.000	0.001	0.001	0.000	0.000	0.000		
Nb	0.000	0.001	0.000	0.001	0.001	0.001	0.001	0.001		
La	0.001	0.002	0.002	0.002	0.000	0.001	0.002	0.000		
Ce	0.000	0.000	0.000	0.002	0.001	0.001	0.000	0.001		
Y	0.001	0.001	0.001	0.001	0.001	0.000	0.001	0.000		
Total	3.000	3.000	3.000	3.000	3.000	3.000	3.000	3.000		
ΣTi+Al+Fe	1.001	0.995	0.991	0.990	0.990	0.989	0.989	0.992		
X_{Al}	0.478	0.256	0.339	0.207	0.320	0.253	0.302	0.276		
F	0.393	0.230	0.250	0.200	0.322	0.229	0.202	0.274		
OH	0.094	0.035	0.094	0.019	0.013	0.033	0.105	0.009		
O	4.512	4.723	4.646	4.768	4.644	4.720	4.673	4.699		
ΣF+OH+O	4.999	4.988	4.990	4.987	4.979	4.982	4.980	4.982		
X_F	0.807	0.868	0.727	0.913	0.961	0.874	0.658	0.968		

The 'high-aluminium' titanite analyses in Table 1 are classified as 'primary' or 'peak' metamorphic, since they are considered to have equilibrated with the assemblage garnet + omphacite + coesite under ultra-high pressure, eclogite-facies conditions. Aluminium contents in these titanites greatly exceed Fe^{3+} contents

TABLE 2. Microprobe analyses and calculated structural formulae to three total cations for secondary titanites in Dabieshan eclogites

Sample Number	CD 18-1	CD 18-1	CD 18-2	CD 18-2	CD 40	CD 40	CD 41	CD 41	CD 74	CD 74
Al_2O_3 content	Max	Min	Max	Min	Max	Min	Max	Min	Max	Min
SiO_2	30.92	30.64	30.74	30.76	31.02	30.98	31.00	30.68	30.95	31.08
TiO_2	38.42	39.25	38.33	39.32	34.78	36.94	33.84	36.84	31.52	35.37
Al_2O_3	1.23	0.91	1.40	0.82	4.13	2.51	4.41	2.29	5.91	3.14
Fe_2O_3	0.48	0.38	0.53	0.42	0.20	0.32	0.33	0.24	0.36	0.48
MnO	0.06	0.10	0.04	0.06	0.00	0.03	0.00	0.03	0.03	0.06
MgO	0.00	0.02	0.01	0.00	0.02	0.02	0.03	0.00	0.03	0.00
CaO	29.36	29.58	29.46	29.37	29.84	29.61	29.84	29.73	29.39	29.70
Na_2O	0.03	0.01	0.01	0.01	0.03	0.05	0.04	0.02	0.02	0.03
K_2O	0.01	0.00	0.02	0.01	0.01	0.01	0.01	0.00	0.01	0.00
ZrO_2	0.06	0.01	0.06	0.07	0.01	0.06	0.06	0.07	0.06	0.07
Nb_2O_5	0.05	0.08	0.07	0.06	0.00	0.00	0.01	0.01	0.02	0.16
La_2O_3	0.18	0.01	0.00	0.18	0.01	0.03	0.18	0.18	0.01	0.17
Ce_2O_3	0.15	0.09	0.04	0.06	0.03	0.14	0.05	0.08	0.03	0.03
Y_2O_3	0.04	0.03	0.10	0.01	0.06	0.06	0.05	0.00	0.06	0.06
F	0.26	0.07	0.24	0.05	1.24	0.85	0.57	0.40	1.64	0.70
Minus O≡F	0.11	0.03	0.10	0.02	0.52	0.36	0.24	0.17	0.69	0.29
Total	101.14	101.15	100.95	101.18	100.86	101.25	100.18	100.40	99.35	100.76
Si	0.993	0.984	0.987	0.989	0.987	0.989	0.988	0.986	0.992	0.993
Ti	0.928	0.948	0.926	0.951	0.832	0.887	0.811	0.891	0.760	0.850
Al	0.047	0.034	0.053	0.031	0.155	0.094	0.166	0.087	0.223	0.118
Fe^{3+}	0.012	0.009	0.013	0.010	0.005	0.008	0.008	0.006	0.009	0.012
Mn	0.002	0.003	0.001	0.002	0.000	0.001	0.000	0.001	0.001	0.002
Mg	0.000	0.001	0.000	0.000	0.001	0.001	0.001	0.000	0.001	0.000
Ca	1.010	1.018	1.014	1.012	1.017	1.013	1.019	1.024	1.009	1.017
Na	0.002	0.001	0.001	0.001	0.002	0.003	0.002	0.001	0.001	0.002
K	0.000	0.000	0.001	0.000	0.000	0.000	0.000	0.000	0.000	0.000
Zr	0.001	0.000	0.001	0.001	0.000	0.001	0.001	0.001	0.001	0.001
Nb	0.001	0.001	0.001	0.001	0.000	0.000	0.000	0.000	0.000	0.002
La	0.002	0.000	0.000	0.002	0.000	0.000	0.002	0.002	0.000	0.002
Ce	0.002	0.001	0.000	0.001	0.000	0.002	0.001	0.001	0.000	0.000
Y	0.001	0.001	0.002	0.000	0.001	0.001	0.001	0.000	0.001	0.001
Total	3.000	3.000	3.000	3.000	3.000	3.000	3.000	3.000	3.000	3.000
ΣTi+Al+Fe	0.987	0.991	0.992	0.992	0.992	0.989	0.985	0.984	0.992	0.980
X_{Al}	0.048	0.034	0.053	0.031	0.156	0.095	0.169	0.088	0.225	0.120
F	0.026	0.007	0.024	0.005	0.125	0.086	0.057	0.041	0.166	0.071
OH	0.032	0.037	0.041	0.036	0.035	0.016	0.116	0.052	0.066	0.059
O	4.924	4.934	4.916	4.943	4.818	4.877	4.800	4.879	4.753	4.848
ΣF+OH+O	4.982	4.978	4.981	4.984	4.978	4.979	4.973	4.972	4.985	4.978
X_F	0.448	0.159	0.369	0.122	0.781	0.843	0.329	0.441	0.716	0.546

and together (Al + Fe^{3+}) show the expected strong negative correlation with Ti content (Fig. 6*a*). Determined fluorine contents are much higher than calculated (OH) contents with values for X_F = F/(F + OH) in the range 0.73–0.96 (Table 1). The positive correlation between F content and (Al + Fe^{3+}) content in Fig. 7*a* confirms that Al substitution in these titanites is strongly coupled to substitution of O^{2-} by F^-. The wider scatter in the correlation in Fig. 7*a* compared to that in Fig. 6*a* at least partly reflects the

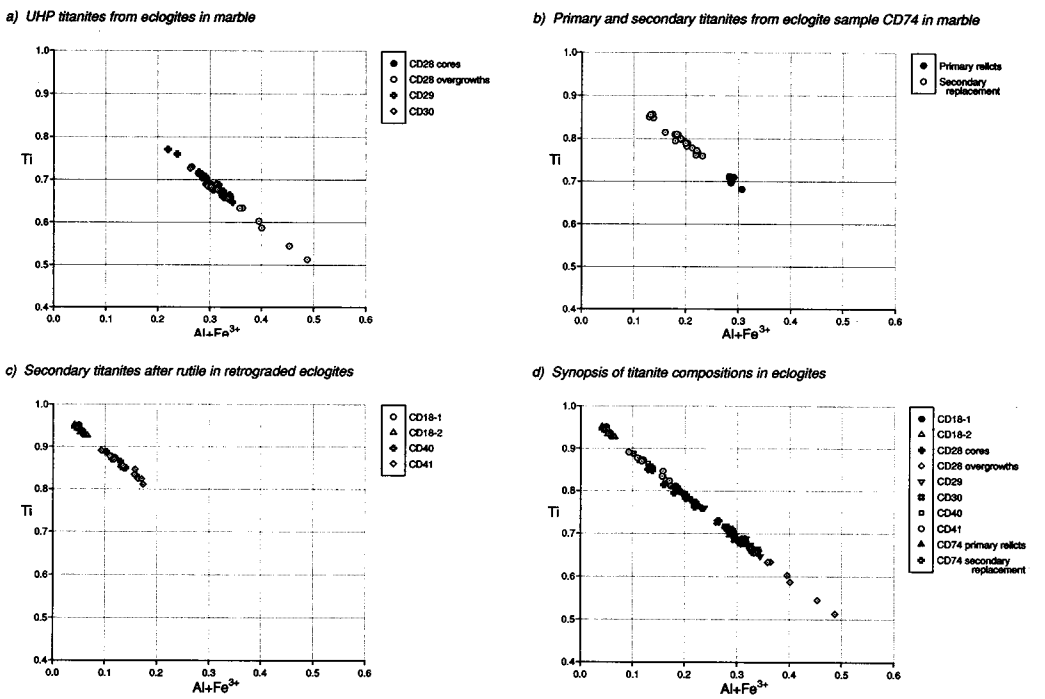

FIG. 6. Ti versus (Al + Fe^{3+}) contents in titanites from eclogites in the Central Dabieshan UHP Eclogite Terrane, China.

greater error brackets which should be attached to the fluorine microprobe analysis figures (see Table 1). The indicated 2σ error bracket of $\pm$ 0.26 wt.% F constitutes a 13% relative error for a value of 2 wt.% F.

From the ranges of analyses listed in Table 1, it is apparent that these UHP titanites in carbonate-bearing eclogites at Shuanghe contain 20.0–39.3 mol.% fluor-titanite component [$Ca(Al,Fe^{3+})FSiO_4$] as against only 0.9–10.5 mol.% hydroxy-titanite component [$Ca(Al,Fe^{3+})(OH)SiO_4$]. The maximum Al content [X_{Al} = Al/(Al + Fe^{3+} + Ti) = 0.478] was recorded in the outer grain overgrowths on the titanites in sample CD28 (see Fig. 2*c–d*), these containing up to 39.3 mol.% fluor-titanite component.

An unusual composition feature of the ultra-high pressure titanites in Dabieshan samples is that they contain low, but detectably significant, contents of Mg and Na. On the other hand, the determined rare earth element contents are insignificant as almost all values are below detection limit.

The compositions of the 'primary' metamorphic titanite relics in sample CD74 (Figs. 6*b*, 7*b*) overlap the composition range of similar generation titanites in samples CD28, 29 and 30 (Figs. 6*a*, 7*a*), whereas the secondary replacement titanites in sample CD74 have similar compositions to those of secondary titanites after rutiles (Figs. 6*c*, 7*c*) in the carbonate-bearing eclogite samples from Guanjialing. The secondary titanites (Table 2), developed during amphibolite-facies retrogression of the various studied eclogite samples, all have significantly lower contents of fluor-titanite component compared to the 'primary' titanites which equilibrated with coesite-bearing eclogite-facies assemblages. The maximum content of fluor-titanite component recorded in the secondary cluster aggregate titanites after rutiles is only 12.5 mol.% and X_F values, indicating the proportion of F^- anions present relative to $(OH)^-$, are mostly much lower.

Determined rare earth element contents in the secondary titanites are negligible, as in the ultra-high pressure titanites, but unlike in the latter there is little indication of significant Mg and Na contents.

Discussion

The highest values determined in this study of titanites for contents of aluminium (X_{Al} = 0.48) and fluor-titanite component (39 mol.%) are somewhat lower than the maximum values of X_{Al} = 0.53 and 53 mol.%

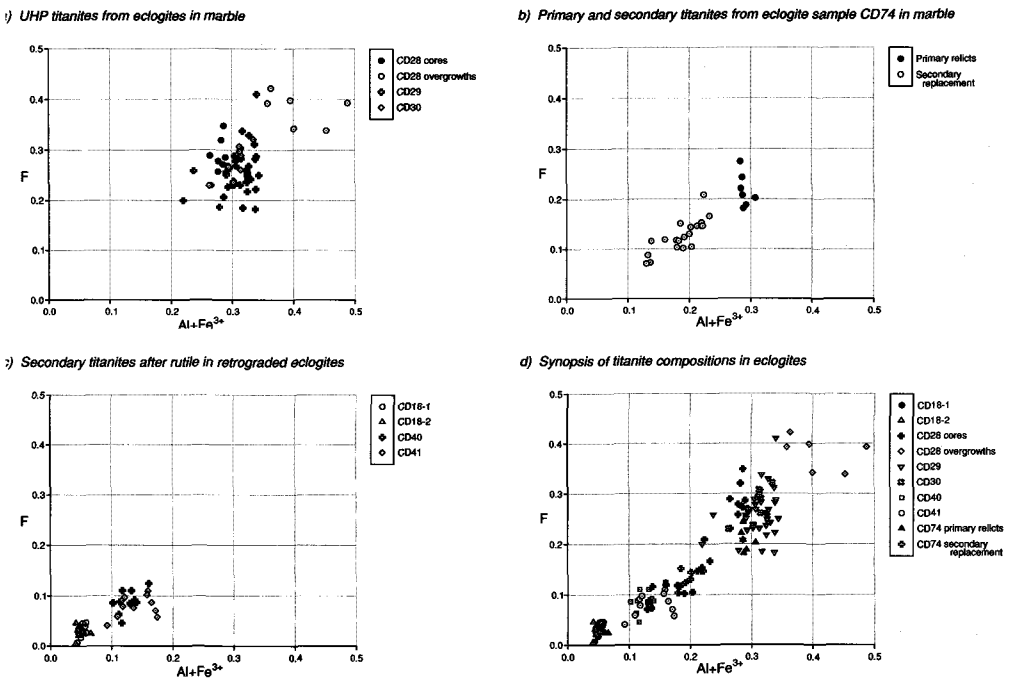

FIG. 7. F versus (Al + Fe^{3+}) contents in titanites from eclogites in Central Dabieshan UHP Eclogite Terrane, China.

recorded by Franz and Spear (1985) in carbonate-bearing eclogites of the Tauern Window, Austria. Note that these values calculated for the quoted analysis for sample no. 79–102 in table II of Franz and Spear (1985) take into account the fact that the published Ti and Al cation values in the calculated structural formula for titanite in that sample have been transposed. Unlike in the Dabieshan eclogites reported in the current study, these Tauern eclogites lack any petrographic evidence that they equilibrated in the coesite stability field. From a consideration of a variety of reaction equilibria both in eclogites and associated high-pressure metasediments, deduced *P–T* conditions for the eclogite-facies metamorphism in the Tauern Window are around 20–22 kbar at 600°C (Franz and Spear, 1983, 1985; Spear and Franz, 1986; Frank *et al.*, 1987; Droop *et al.*, 1990). By contrast the primary titanite and coesite-bearing assemblages of the Central Dabieshan UHP Eclogite Terrane are deduced to have equilibrated at a minumum pressure of 27–28 kbar at temperatures of *ca.* 700±50°C (Carswell *et al.*, 1993; Cong *et al.*, 1995; Wang and Liou, 1993).

It is clear from petrographic observations, as well as crystal chemical considerations (Oberti *et al.*, 1991) and experimental data (Smith, 1981), that $Al^{VI}FTi_{-1}O_{-1}$ substitution in titanites is favoured by high pressures and low temperatures. However, the higher contents of fluor-titanite component in titanites in some eclogites from the Tauern Window, compared to those reported here in coesite-bearing samples from Central Dabieshan, caution against use of this composition parameter as a qualitative, let alone quantitative, indicator of pressure-temperature conditions of metamorphism. This study, as also that by Franz and Spear (1985), demonstrates that a crucial constraint on this substitution must be imposed by the F activity in the fluid phase promoting metamorphic equilibration. Both studies describe certain titanite grains with growth zones (e.g. Fig. 2*c–d* in this study) of markedly different Al (and F) contents. This compositional zonation seems most reasonably attributed to variations in the fluorine activity of the fluid phase present during titanite growth under high pressure conditions.

Examples of reaction equilibria which may control the stability of titanite relative to rutile in such carbonate-bearing, excess silica, eclogites include:

Rutile + calcite/aragonite + quartz/coesite = titanite + CO_2

and

Rutile + grossular + quartz/coesite + H_2O = titanite + zoisite

(high pressure assemblages on left-hand sides of both equations)

High H_2O fluid activity will thus favour the stability of titanite + zoisite/clinozoisite – an assemblage commonly stabilised under retrograde amphibolite-facies conditions during exhumation of these and other eclogites.

Under water-deficient eclogite-facies conditions, high CO_2 fluid activity will favour the stability of rutile + carbonate rather than titanite. However, enhanced F activity in the fluid phase could be expected to promote the stability of fluor-titanite relative to rutile + carbonate under high-pressure conditions. Thus the crystallization sequence of firstly rutile then titanites with increasing fluor-titanite component, as seem for example in sample CD28, may simply reflect decreasing CO_2 activity and increasing fluorine activity in the available fluid phase, rather than changing P–T conditions, during the ultra-high pressure metamorphism of these carbonate-bearing eclogites at Shuanghe in Dabieshan.

Acknowledgements

This study is part of a collaborative research project between geoscientists at the Universities of Sheffield and Leicester in the United Kingdom and Academia Sinica in Beijing, China. Financial support for the study from the Royal Society in the United Kingdom and the National Natural Sciences Foundation of China is gratefully acknowledged.

References

Berman, R.G. (1988) Internally-consistent thermodynamic data for minerals in the system Na_2O–K_2O–CaO–MgO–FeO–Fe_2O_3–Al_2O_3–SiO_2–TiO_2–H_2O–CO_2. *J. Petrol.*, **29**, 445–522.

Carswell, D.A., Wilson, R.N., Cong, B., Zhai, M. and Zhao, Z. (1993) Areal extent of the ultra-high pressure metamorphism of eclogites and gneisses in Dabieshan, central China. *Terra Abstracts* (*Terra Nova* 5), No. 4, 5.

Cong, B., Zhai, M., Carswell, D.A., Wilson, R.N., Qingchen, W., Zhai, Z. and Windley, B.F. (1995) Petrogenesis of ultrahigh-pressure rocks and their country rocks at Shuanghe in Dabieshan, central China. *Eur. J. Mineral.*, **7**, 119–38.

Deer, W.A., Howie, R.A. and Zussman, J. (1992) *An Introduction to the Rock-forming Minerals*. 2nd Ed. Longman.

Droop, G.T.R., Lombardo, B. and Pognante, U. (1990) Formation and distribution of eclogite facies rocks in the Alps. In *Eclogite Facies Rocks* (D.A. Carswell, ed.), Blackie, Glasgow, 225–59.

Enami, M., Suzuki, K., Liou, J.G. and Bird, D.K. (1993) Al-Fe^{3+} and F-OH substitutions in titanite and constraints on their P-T dependence. *Eur. J. Mineral.*, **5**, 219–31.

Franz, G. and Spear, F.S. (1983) High pressure metamorphism of siliceous dolomites from the central Tauern Window, Austria. *Amer. J. Sci.*, **283A**, 396–413.

Franz, G. and Spear, F.S. (1985) Aluminous titanite (sphene) from the eclogite zone, south-central Tauern Window, Austria. *Chem. Geol.*, **50**, 33–46.

Frank, W., Höck, V. and Miller, C. (1987) Metamorphic and tectonic history of the central Tauern Window. In *Geodynamics of the Eastern Alps* (H.W. Flugel and P. Faupl, eds.), Deuticke, Vienna, 34–54.

Hirajima, T., Zhang, R., Li, J. and Cong, B. (1992) Petrology of the nyboite-bearing eclogite in the Donghai area, Jiangsu province, eastern China. *Mineral. Mag.*, **56**, 37–46.

Manning, C.E. and Bohlen, S.R. (1991) The reaction titanite + kyanite = anorthite + rutile and titanite-rutile barometry in eclogites. *Contrib. Mineral. Petrol.*, **109**, 1–9.

Mottana, A., Carswell, D.A., Chopin, C. and Oberhansli, R. (1990) Eclogite facies mineral parageneses. In *Eclogite Facies Rocks* (D.A. Carswell, ed.), Blackie, Glasgow, 14–52.

Oberti, R., Smith, D.C., Rossi, G. and Caucia, F. (1991) The crystal-chemistry of high-aluminium titanites. *Eur. J. Mineral.*, **3**, 777–92.

Smith, D.C. (1977) Aluminium bearing sphene in eclogites from Sunnmöre (Norway). *Geologynytt*, **10**, 32–3.

Smith, D.C. (1981) The pressure and temperature dependence of Al-solubility in sphene in the system Ti–Al–Ca–Si–O–F. *Progr. Experim. Petrol. N.E.R.C. Publication Series*, **D-18**, 193–7.

Smith, D.C. (1988) A review of the peculiar mineralogy of the 'Norwegian coesite-eclogite province', with crystal-chemical, petrological, geochemical and geodynamical notes and an extensive bibliography. In: *Eclogites and Eclogite-Facies Rocks* (D.C. Smith, ed.), Elsevier, 1–206.

Spear, F.S. and Franz, G. (1986) P-T evolution of metasediments from the Eclogite Zone, south-central Tauern window, Austria. *Lithos*, **19**, 219–34.

Sobolev, N.V. and Shatsky, V.S. (1990) Diamond inclusions in garnets from metamorphic rocks: a new environment for diamond formation. *Nature*, **343**, 742–6.

Wang, X. and Liou, J.G. (1993) Ultra-high-pressure metamorphism of carbonate rocks in the Dabie Mountains, central China. *J. metam. Geol.*, **11**, 75–88.

[*Manuscript received 15 March 1995: revised 16 May 1995*]